

## **REMARKS**

Favorable reconsideration is respectfully requested in view of the foregoing amendments and the following remarks.

### **I. CLAIM STATUS AND AMENDMENTS**

Claims 1-19 were pending in this application when last examined.

Claims 1-9, 14, 17 and 19 were withdrawn as non-elected subject matter.

Claims 10-13, 15-16 and 18 are rejected.

Claims 11 and 13 are cancelled without prejudice or disclaimer thereto.

Claim 10 is amended to correct dependency on a withdrawn claim and to clarify the claimed invention. Support can be found on page 5, lines 28-29, page 6, lines 28-29 and claims 4 and 13 as filed.

Claim 12 is amended to clarify the claimed invention.

No new matter has been added.

The Examiner is respectfully requested to note that in response to the restriction requirement of June 24, 2009, the Applicants elected "antibody" as the species. It was the Examiner's opinion as expressed in the Office Action of November 6, 2009 as well as in the February 17, 2010 interview that such species does not include within its scope anti-CXCR3 ligand antibody. Applicants disagree with the Examiner's conclusion and respectfully reserve the right to file a petition with regard to the Examiner's determination. Furthermore, Applicants respectfully ask that anti-CXCR ligand antibody be examined upon allowance of the elected species.

### **II. CLAIM OBJECTION**

On page 3 of the Office Action, claims 10-13, 15-16 and 18 were objected to for the noted reasons. This objection is overcome, as applied to amended claims, for reasons which are self-evident.

### **III. ENABLEMENT REJECTION**

On pages 3-6, claims 10, 13, 15-16 and 18 were rejected under 35 U.S.C. § 112, first paragraph, because the specification, while being enabling for a method of treating or preventing lymph node metastasis of CXCR3 expressing cancers comprising intestine cancer, breast and melanoma cancers comprising administering anti-CXCR3 antagonist antibody, does not reasonably provide enablement for the full scope of the claims drawn to treating a cancer or preventing metastasis of any cancer that includes the cancer cells not expressing the CXCR3 protein.

It is noted that claim 10, the only independent claim under examination, is amended without acquiescence to recite CXCR3-expressing cancer. Thus, the claims have been amended as indicated as enabled by the Examiner. Thus, Applicants respectfully request withdrawal of this rejection.

### **IV. ART REJECTIONS**

On pages 6-7, claims 10-12, 15, 16 and 18 were rejected under 35 U.S.C. § 102(b) as anticipated by Burns et al. (US 2003/0124628). Further, on pages 7-9, claims 10-13, 15, 16 and 18 were rejected under 35 U.S.C. § 103(a) as unpatentable over Burns et al. in view of Blake Cady (Arch. Surg., 1984).

Applicants respectfully traverse these rejections.

Blake Cady describes that cancer metastasizes to lymph node. Burn et al. suggests that chemokine is involved in cancer metastasis and mentions CXCR3 as one of chemokine receptors. The examiner alleged that the present invention was obvious for a person skilled in the art in front of Blake Cady and Burn et al.

Applicants respectfully disagree with the Examiner. Burn et al. describes that CXCR4 was shown to be involved in breast cancer metastasis (see, paragraphs 0007, 0211). Burn et al. however, does not specifically mention CXCR3 in relation to cancer metastasis.

It should be noted that the chemokine involved in cancer metastasis depends on the organ to which cancer metastasizes. The claimed invention is based on the finding that CXCR3 is involved in lymph node metastasis. Examples of the specification demonstrate that CXCR3 does not affect metastasis to lung and liver (see page 45, Table 3 of the specification).

Also, attached hereto is a reference showing that involvement of chemokine in cancer metastasis is not so simple. The reference shows that CXCR4, but not CXCR7, is involved in liver and lung cancer metastasis (see page 1245 as well as Fig. 4 and Table 2 of Attachment A).

Thus, Burn et al. does not disclose or suggest to a skilled artisan involvement of CXCR3 in lymph node metastasis. Therefore, a person skilled in the art could not achieve the claimed invention even combining Burn et al. and Blake Cady.

Thus, for the above-noted reasons, these rejections are untenable and should be withdrawn.

On page 9-11, claims 10-13, 15, 16 and 18 were rejected under 35 U.S.C. § 103(a) as unpatentable over Robledo et al. (JBC, 2001), or Kawada et al. (Cancer Res., 2004), or Goldberg-Bittman et al. (Immu. Let., May 29, 2004) in view of Levanon et al. (US 2005/0152906).

Attached herewith is a verified English translation of Japanese Priority Application No. 2004-065612 which was filed March 9, 2004. Thus, priority of the present application is perfected. Kawada et al, Gold-Bittman et al. and Levanon et al. can no longer be properly applied at prior art references. Thus, this rejection is untenable and should be withdrawn.

**CONCLUSION**

In view of the foregoing amendments and remarks, it is respectfully submitted that the present application is in condition for allowance and early notice to that effect is hereby requested.

If the Examiner has any comments or proposals for expediting prosecution, please contact the undersigned attorney at the telephone number below.

Respectfully submitted,

Makoto TAKETO et al.

William R.  
By **Schmidt, II**  
William R. Schmidt, II  
Registration No. 58,327  
Attorney for Applicants

Digitally signed by William R.  
Schmidt, II  
DN: cn=William R. Schmidt, II, o, ou,  
email=bschmidt@wenderoth.com,  
c=US  
Date: 2010.05.06 13:47:51 -04'00'

WRS/vah  
Washington, D.C. 20005-1503  
Telephone (202) 721-8200  
Facsimile (202) 721-8250  
May 6, 2010

## BASIC-LIVER, PANCREAS, AND BILIARY TRACT

### CXCR4 Expression Increases Liver and Lung Metastasis in a Mouse Model of Pancreatic Cancer

DIETER SAUR,\* BARBARA SEIDLER,\* GÜNTER SCHNEIDER,\* HANA ALGÜL,\* ROSWITHA BECK,† REINGARD SENEKOWITSCH-SCHMIDTKE,† MARKUS SCHWAIGER,† and ROLAND M. SCHMID\*

\*Department of Internal Medicine 2 and †Department of Nuclear Medicine, Technical University of Munich, Munich, Germany

See editorial on page 1344.

**Background & Aims:** Expression of the G $\alpha$ -protein-coupled chemokine receptor CXCR4 has recently been linked to increased proliferation, invasion, and migration of human pancreatic cancer cell lines. However, the relevance of CXCR4 for organ-specific pancreatic cancer metastasis in vivo remains unclear. Here, we have studied the role of CXCR4 in vivo using noninvasive imaging of targeted metastasis in a mouse model of pancreatic cancer. **Methods:** Functional expression of the chemokine receptors CXCR4 and CCR7 was achieved by stable transfection of murine TD-2 pancreatic cancer cells and analyzed by flow cytometry, calcium flux, migration, and proliferation assays. The metastatic potential of the different stable TD-2 cell clones was assessed by tail vein metastatic assays in nude mice using in vivo bioluminescent imaging. **Results:** Native TD-2 cells display very low abundant CXCR4 and CCR7 expression and show poor metastatic potential after tail vein injection. To study the role of CXCR4 in pancreatic cancer metastasis, we selected stable TD-2 cell clones with similar CXCR4 expression levels as human pancreatic cancer cell lines derived from metastatic lesions. CXCR4, but not CCR7, expression dramatically increased the in vivo metastatic potential of TD-2 cells, resulting in liver and lung metastasis in nude mice. Systemic administration of the selective CXCR4 inhibitor AMD 3100 effectively blocked the enhanced metastatic potential of CXCR4-expressing pancreatic cancer cells. **Conclusions:** These results indicate that CXCR4 expression mediates organ-specific metastasis of pancreatic cancer cells and provide preclinical evidence that blockade of the CXCL12/CXCR4 axis is a target for antimetastatic therapy.

of cancer death in the Western world.<sup>1,2</sup> This poor prognosis with a median survival time of only 6 months is mainly caused by extensive local infiltration, as well as early lymphatic and hematogenous metastasis. At the time of diagnosis, >80% of the patients have locally advanced or metastatic disease.<sup>3</sup> Because of the resistance against all forms of conventional therapy, management of these patients focuses currently solely on palliation. Even when discovered at an early stage without signs of local infiltration and metastasis, long-term survival after curative surgical resection is rare, with a 5-year survival rate of ~20%.<sup>4</sup> This indicates that pancreatic cancer is a micrometastatic disease.

Because metastasis plays the major role in morbidity and mortality of pancreatic cancer, understanding biology and genetics of the metastatic process will be crucial to improve treatment and clinical outcome. Metastasis is a nonrandom, highly organ-specific pathophysiologic process.<sup>5-8</sup> It involves multiple steps and numerous interactions between cancer cells and the host, such as proliferation, induction of angiogenesis, invasion, detachment of the tumor cells from the primary tumor, invasion into lymph and blood vessels, survival in the circulation, and extravasation into target organs and, there again, proliferation and induction of angiogenesis.<sup>7,9</sup>

Pancreatic cancer metastatic dissemination occurs by lymphatic and hematogenous pathways. Metastatic lesions are found stereotypically in regional lymph nodes. The hematogenous spread is most often found in liver and lung. Although some molecules have been implicated in pancreatic cancer metastasis in vitro and in vivo, little is known about the detailed mechanism

**Abbreviations used in this paper:** fLuc, firefly luciferase; PE, phycoerythrin; RLU, relative light units; RT-PCR, reverse transcriptase polymerase chain reaction.

© 2005 by the American Gastroenterological Association

0016-5085/05/\$30.00

doi:10.1053/j.gastro.2005.06.056

Pancreatic ductal adenocarcinoma with an incidence of 1 in 10,000 people per year has a 5-year survival rate of less than 5%, making it the fourth leading cause

of organ-specific tumor metastasis. In particular, mechanisms of targeted liver and lung metastasis, as key prognostic factors for pancreatic carcinoma, are unclear, illustrating the need to find new target molecules leading to the homing of pancreatic cancer cells to specific organs.<sup>10</sup>

Recently, organ-specific metastasis has been linked to interactions between chemokine receptors on cancer cells and matching chemokines in target organs.<sup>11</sup> Chemokines, initially described as regulators of leukocyte trafficking, belong to the superfamily of small molecule cytokines. They mediate chemotaxis through binding to Gi-protein-coupled receptors leading to the induction of cytoskeletal rearrangements, increased adhesion, and migration to specific anatomical sites.<sup>12–14</sup> Gradients of the chemokine stromal cell-derived factor 1 $\alpha$  (SDF1 $\alpha$  or CXCL12) are proposed to attract CXCR4-positive tumor cells to specific metastatic sites analogous to the directed homing of leukocytes. High amounts of CXCL12 are produced from organs commonly affected by cancer metastasis, such as lung and liver.<sup>15</sup> Malignant cells that express the cognate receptor CXCR4 migrate into these organs, evade the circulation, and form metastatic tumors.

The CXCL12/CXCR4 axis plays an important role in experimental hematogenous metastasis models of breast, prostate, colon cancer, and melanoma in vivo.<sup>15–20</sup> In contrast, expression of the chemokine receptor CCR7 accelerates lymph node metastasis of melanoma.<sup>21</sup>

In pancreatic cancer cell lines and primary tumors, expression of CXCR4 has been described previously.<sup>22–24</sup> In addition, a recent study showed substantially higher expression levels of CXCR4 in human pancreatic cancer cell lines derived from metastatic lesions compared with those derived from primary tumors.<sup>24</sup> So far, the relevance of CXCR4 expression levels for organ-specific pancreatic cancer metastasis in vivo remains unclear.

Here, we have studied the role of CXCR4 expression in vivo using bioluminescent imaging of targeted metastasis in a mouse model of pancreatic cancer. TD-2 cells, derived from the primary pancreatic tumor of a transforming growth factor (TGF)- $\alpha$ /p53<sup>+/-</sup> mouse,<sup>25,26</sup> express minimal amounts of CXCR4 and display poor metastatic potential. Expression of CXCR4 dramatically increases the metastatic potential of TD-2 cells in vivo, resulting in the formation of liver and lung metastasis in nude mice. The increased metastatic potential of CXCR4-expressing pancreatic cancer cells could be blocked by systemic administration of the selective CXCR4 inhibitor AMD 3100, demonstrating that blockade of the CXCL12/CXCR4 axis is a promising new target for antimetastatic therapy.

## Materials and Methods

### Materials

All cell culture reagents were obtained from Invitrogen (Groningen, The Netherlands). Primers were made by MWG (Ebersberg, Germany), and restriction endonucleases were obtained from New England Biolabs (Mannheim, Germany). The *Escherichia coli* strain TOP10 (Invitrogen) was used for transformation and plasmid amplification.

### Tissue Preparation and RNA Isolation

Tissue specimens and cultured cells were cleaned with phosphate-buffered saline (PBS) and total RNA was isolated exactly as described using the isothiocyanate/phenol/chloroform method.<sup>27,28</sup>

### Reverse Transcriptase Polymerase Chain Reaction

Reverse transcription (RT) and polymerase chain reaction (PCR) amplification was carried out as described previously.<sup>28,29</sup> RT-PCR was performed with specific primer pairs spanning the coding sequences of murine CXCR4 and CCR7 (for primers see Table 1) for 30 cycles using a proofreading polymerase (PfuUltra; Stratagene, Amsterdam, The Netherlands) and oligo-dT primed cDNA from mouse thymus (annealing, 58°C, 30 seconds; extension, 72°C, 90 seconds; denaturation, 94°C, 30 seconds). Amplification products were cloned and subjected to DNA sequence analysis (GATC, Konstanz, Germany).

### Quantitative Real-Time RT-PCR

Real-time quantitative RT-PCR analyses were carried out using an ABI PRISM 7700 Sequence Detection System instrument with Sybr Green as fluorescent dye (Applied Biosystems, Weiterstadt, Germany). cDNA samples for quantitative analysis were generated with the TaqMan Reverse Transcription Reagents (Applied Biosystems) as recommended by the manufacturer, using MuLV reverse transcriptase; random hexamer primers; and 5  $\mu$ g total RNA from the different tissues, tumors, metastases, and cell lines. CXCR4, CCR7, CXCL12, CCL19, CCL21, and firefly luciferase (fLuc) transcripts were amplified with primers designed to meet specific criteria by using the Primer Express software (Applied Biosystems). Sequences of primers used in the study are shown in Table 1. As endogenous reference, the globally expressed housekeeping gene cyclophilin was used as described previously.<sup>30</sup> The principle of real-time RT-PCR has been described.<sup>29,31</sup> For each amplicon, the amount of target and endogenous reference was determined from a standard curve generated by serial 5-fold dilutions (625,000 to 8 copies) of plasmids containing the respective target sequence. The standard curve was amplified in triplicate during every experiment, and the amount of target gene was normalized by the endogenous reference. Quantitative PCR was performed using Sybr Green TaqMan Universal PCR Master Mix (Applied Bio-

**Table 1.** Sense and Antisense Strand Primers

Name	Sequence	
	5'	3'
mCXCR4-ATG <i>Xba</i> I (S)	GCTCTAGAGTTTAAACGCCGCCATGGAACCGATCAG	
mCXCR4-ATT <i>Xba</i> I (AS)	GCTCTAGACCTGCAGGGTTTAAACCTTAGCTGGAGTGAAAAGTGGAGGA	
mCCR7-ATG <i>Xba</i> I (S)	GCTCTAGAGTTTAAACGCCACCATGGACCCAGGGAAAC	
mCCR7-TGA <i>Xba</i> I (AS)	GCTCTAGACCTGCAGGGTTTAACTCACTACGGGGAGAAGGTTGTGG	
mCXCR4-TaqMan (S)	GCTGGCTGAAAAGGCAGTCTAT	
mCXCR4-TaqMan (AS)	TGACGTCGGCAAAGATGAAGT	
mCXCL12-TaqMan (S)	CCAGAGCCAACGTCAAGCAT	
mCXCL12-TaqMan (AS)	CAGCCGTGCAACAATCTGAA	
mCCR7-TaqMan (S)	ACCATGGACCCAGGGAAAC	
mCCR7-TaqMan (AS)	GGTATTCTCGCCGATGTAGTCAT	
mCCL19-TaqMan (S)	GGTGCTAATGATGCGGAAGAC	
mCCL19-TaqMan (AS)	ATAGCCCCCTTAGTGTGGTGAACA	
mCCL21-TaqMan (S)	TGAACAGACACAGCCCTCAAGA	
mCCL21-TaqMan (AS)	CCTCTTTGCCTGTGAGTTGGA	
Cyclophilin-TaqMan (S)	ATGGTCAACCCACCGTGT	
Cyclophilin-TaqMan (AS)	TTCTGCTGTCTTTGGAACTTTGTG	
fLuc-TaqMan (S)	TCTCTAAGGAAGTGTGGTTG	
fLuc-TaqMan (AS)	GGCTGTGTCTAGAAGTGACG	
hCXCR4-TaqMan (S)	GCATGACGGACAAGTACAGGCT	
hCXCR4-TaqMan (AS)	AAAGTACCAGTTGCCACGGC	

S, sense; AS, antisense.

systems), cDNA corresponding to 100 ng total RNA and 300 nmol/L primers in a 25  $\mu$ L final reaction mix (1 PCR cycle, 50°C, 2 minutes, 95°C, 10 minutes; 40 PCR cycles, 60°C, 1 minute, 95°C, 15 seconds). Signals were analyzed by the ABI Prism Sequence Detection System software version 1.7 (Applied Biosystems).

### Plasmid Constructions

The coding sequences of murine CXCR4 and CCR7 were amplified by RT-PCR, cut with *Xba*I and cloned sticky end into the *Xba*I site of the multiple cloning site B of the plasmid pIRES (BD Clontech, Heidelberg, Germany). To generate bicistronic vectors for concomitant expression of fLuc and CXCR4 or CCR7 by using an internal ribosome entry site (IRES), the coding sequence of fLuc was removed from pGL3-basic (Promega, Mannheim, Germany) by restriction endonuclease digestion with *Hind*III and *Xba*I, gel purified, blunted, and ligated into the blunted *Xba*I site of the multiple cloning site A of pIRES, resulting in the plasmids pIRES-fLuc-CXCR4 and pIRES-fLuc-CCR7, respectively. To generate a monocistronic fLuc expression vector, the IRES element and the CXCR4 coding sequence were removed from pIRES-fLuc-CXCR4 by digestion with *Mlu*I and *Not*I, followed by blunting and religation (pIRES-fLuc). Integrity of all cloned sequences was confirmed by automated DNA sequencing (GATC, Konstanz, Germany) using an ABI Prism 377 DNA sequencer (Applied Biosystems).

### Cell Lines

Human pancreatic cancer cell lines derived from primary tumors (MiaPaCa2, Panc1) and from metastatic lesions (Capan1, Hs766T) were purchased from the American Type

Culture Collection (Manassas, VA). Generation of TD-2, a murine ductal pancreatic tumor cell line from the pancreatic carcinoma of a TGF- $\alpha$ /p53<sup>+/-</sup> mouse has been described previously.<sup>25,26</sup> TD-2 cells were cultured with RPMI 1640 medium, and MiaPaCa2, Panc1, Capan1, and Hs766T were maintained in DMEM medium (37°C, 5% CO<sub>2</sub>). All media contained 10% fetal calf serum (FCS), 2 mmol/L L-glutamine, 100 U/mL penicillin, and 100  $\mu$ g/mL streptomycin sulfate.

### Stable Transfection of Cell Lines

TD-2 cells were stably transfected with the bicistronic expression vectors pIRES-fLuc-CXCR4 and pIRES-fLuc-CCR7 or the monocistronic vector pIRES-fLuc under the control of the cytomegalovirus promoter by using Effectene (Qiagen, Hilden, Germany), according to the manufacturer's instructions. Stable fLuc/CXCR4, fLuc/CCR7, and, as control, fLuc-expressing TD-2 cell clones were selected by treatment with 1000  $\mu$ g/mL active Geneticin.

### Luciferase Assay

Stable TD-2 clones and mouse tissues were homogenized in lysis buffer (Promega). Total cellular protein was determined by Bio-Rad II assay (Bio-Rad, Hercules, CA), and fLuc activity was measured in a luminometer (EG&G Berthold, Bad Wildbad, Germany) by using a Luciferase Reporter Assay System (Promega) as previously described.<sup>29,31</sup> All values were determined from 3 independent experiments and are expressed as mean values  $\pm$  standard deviation (SD). FLuc activity was normalized in all samples for total protein content. Data are presented as relative light units of fLuc/ $\mu$ g protein.

### Flow Cytometry

Human and murine pancreatic cancer cells were harvested from tissue culture flasks, washed with PBS, and resuspended in ice-cold PBS containing 1% FCS. TD-2 cells were incubated with 20  $\mu\text{g/mL}$  phycoerythrin (PE)-conjugated rat anti-mouse CXCR4 monoclonal antibody (clone 2B11, BD Pharmingen), 20  $\mu\text{g/mL}$  goat anti-mouse CCR7 polyclonal antibody (M-18; Santa Cruz Biotechnologies, Heidelberg, Germany), or isotype controls for 60 minutes at 4°C. TD-2 cells labeled with anti-mouse CCR7 antibody or isotype control were then stained with FITC-conjugated anti-goat IgG (MP Biomedicals, Eschwege, Germany) for 60 minutes at 4°C. The human pancreatic cancer cell lines MiaPaCa2, Panc1, and Hs766T were incubated with 10  $\mu\text{g/mL}$  PE-labeled mouse anti-human CXCR4 antibody (clone 12G5; BD Pharmingen) or an isotype control for 60 minutes at 4°C. Ten thousand cells were analyzed with FACScalibur flow cytometer and CellQuest software (both from BD Pharmingen).

### Ca<sup>2+</sup> Mobilization

Ca<sup>2+</sup>-mobilization in response to CXCL12 was measured using a fluorescence multiwell plate reader equipped with dual injectors (FLUOstar Optima, BMG Labtechnologies, Offenburg, Germany) as described by Lin et al.<sup>32</sup> Adherent cells were grown overnight on clear-bottom, black-walled, 96-well plates (Greiner Bio-One, Frickenhausen, Germany), loaded with 4  $\mu\text{mol/L}$  Fluo-3AM (Invitrogen) for 60 minutes at 37°C, and the change of fluorescence intensity (excitation wavelength, 485; emission wavelength, 530) was followed kinetically after injection of CXCL12 or CCL21 (R&D Systems, Minneapolis, MN).

### Chemotaxis Assay

Cell migration was evaluated using transwell plates (24-well format, 8- $\mu\text{m}$  pores size; BD Falcon). Cells were resuspended at  $1 \times 10^6/\text{mL}$  in medium supplemented with 1% FCS, and  $5 \times 10^5$  cells were seeded in the upper chamber. Recombinant CXCL12 or CCL21 (R&D Systems) in medium containing 1% FCS were used as chemoattractants in the lower compartment. The chambers were incubated overnight at 37°C. Cells on the upper surface of the membrane were removed using a cotton-wool swab. Migrated cells on the lower surface were stained with crystal violet, and the number of migrated cells were counted in 5 medium power fields (magnification,  $\times 100$ ). Results are expressed as the mean number of net migrated cells  $\pm$  SD. Each experiment was done in triplicate.

### Cell Proliferation Assay

Proliferation was measured in vitro using a BrdU cell proliferation ELISA (Roche, Mannheim, Germany);  $2 \times 10^3$  cells/well were plated on flat-bottomed 96-well plates. After 24 hours, cells were maintained in medium with 10%, 1%, and 0% FCS and stimulated with PBS or 100 ng/mL CXCL12  $\pm$  1  $\mu\text{g/mL}$  AMD 3100 (Sigma, Deisenhofen, Germany) for

24 hours. The pyrimidine analogue 5-bromo-2'-deoxyuridine (BrdU) was added to the cells for an additional time of 2 hours, and the cells were subsequently treated according to the manufacturer's instructions. BrdU incorporation was measured by a colorimetric assay at 370 nm (reference wavelength, 492 nm) in a plate spectrophotometer. Results are expressed as mean of the absorbance ( $A_{370\text{nm}} - A_{492\text{nm}}$ ) of stimulated and unstimulated cells  $\pm$  SD from 3 independent experiments in triplicate.

### MTT Assay

Cell viability was analyzed using the Cell Proliferation Kit I (MTT; Roche) as recommended by the manufacturer. Cells were seeded on 96-well plates at  $2 \times 10^3$  cells/well. After 24, 48, and 72 hours, cells were incubated for 4 hours with 0.5 mg/mL MTT dye in complete cell culture medium. After solubilization of the purple formazan crystals, absorbance was measured at 570 nm (background wavelength, 650 nm) using a plate spectrophotometer.

### Experimental Metastasis Assay

Six-week-old female nude mice (Charles River, Sulzbach, Germany) were used in standard tail vein metastatic assay as described by Elkin and Vlodavsky.<sup>33</sup> Stable TD-2 clones were harvested from culture flasks by incubation with trypsin for 2–3 min. Only single-cell-suspensions with a cell viability of  $>95\%$ , as determined by trypan blue exclusion, were used for intravenous (IV) injection. One  $\times 10^6$  tumor cells were injected into the lateral tail vein using a 27-gauge needle. Mice were killed when metastasis was detected by in vivo bioluminescence imaging or after 120 days, and tissues were examined macroscopically and microscopically for occurrence of metastases. All animal experiments were approved by the local authorities and in compliance with the institution's guidelines.

### In Vivo Bioluminescence Imaging

Mice were anesthetized with ketamine/xylazine, injected with D-luciferin (Synchem, Kassel, Germany) at 150 mg/kg intraperitoneally (IP) and imaged after 10 minutes using a cooled back-thinned, charge-coupled device camera (OrcaII ER, Hamamatsu, Hersching, Germany) equipped with an image intensifier for 10–120 seconds; bin size, 2; gain, 700. A photographic grayscale image was taken, and the bioluminescent signals were displayed in pseudocolors and projected on the grayscale image using SimplePCI software (Hamamatsu).

### In Vivo AMD 3100 Treatment

Mice were treated with AMD 3100 (subcutaneous injection of 1.25 mg/kg twice per day) or PBS for 10 days. Cohorts of 7 mice were used per experiment.

### Immunostaining

Formalin-fixed, paraffin-embedded mice tissue sections were mounted on 3-amino-propyltriethoxysilane-coated slides. Dewaxed paraffin sections were placed in a microwave



(10 minutes, 600 watts) to recover antigens before staining. Antibodies used were as follows: goat anti-mouse CXCR4 polyclonal antibody (1:750, No. 201-819, Alexis Biochemicals), mouse anti-PCNA antibody (1:250, PC-10, Santa Cruz Biotechnologies), followed by secondary antibodies conjugated to biotin. Peroxidase-conjugated streptavidin was used with 3,3'-diaminobenzidine tetrahydrochloride (DAB; Sigma) as chromogen for detection. Hematoxylin was used for nuclear and eosin for cytoplasmatic counterstaining.

### Data Analysis

Unless otherwise indicated, all data were determined from 3 independent experiments, each done in triplicate, and expressed as mean values  $\pm$  SD. Comparisons among data sets were made with analysis of variance, followed by Student *t* test or Mann-Whitney rank sum test. For multiple testing, a Bonferroni correction of the *P* values was made. Chi-square and Fisher exact tests were used to compare the frequencies of metastasis between the different groups using StatXact-4.0.1 software (Cytel Software corporation, Cambridge, MA), as described previously.<sup>31</sup> Values of *P* < .05 (2-tailed) were considered to be statistically significant.

## Results

### Expression of the Chemokine Receptors CXCR4 and CCR7 and Their Ligands in Murine Tissues and TD-2 Pancreatic Cancer Cells

To investigate mRNA expression profiles of CXCR4, CXCL12, CCR7, CCL19, and CCL21 in the mouse, diverse tissues were analyzed by quantitative RT-PCR. As expected, CXCR4 mRNA expression levels were highest in lymph nodes, thymus, and spleen, whereas only minimal amounts were present in brain, colon, and the murine pancreatic cancer cell line TD-2, with  $\sim$ 30 copies per 100 ng total RNA (Figure 1A). CXCL12, the only known ligand of CXCR4, was highly expressed in liver, lung, lymph nodes, kidney, and heart. Interestingly, TD-2 cells showed moderate expression levels of CXCL12 (Figure 1B). Pancreas, lymph nodes, thymus, and spleen displayed highest expression of CCR7, whereas only trace amounts were present in TD-2 cells (Figure 1C). Expression of the CCR7 ligands CCL19 and CCL21 was highly abundant in lymph nodes (Figure 1D and E), as described in human tissues.<sup>15</sup>

### Stable Expression of FLuc and Functional CXCR4 and CCR7 in TD-2 Cells

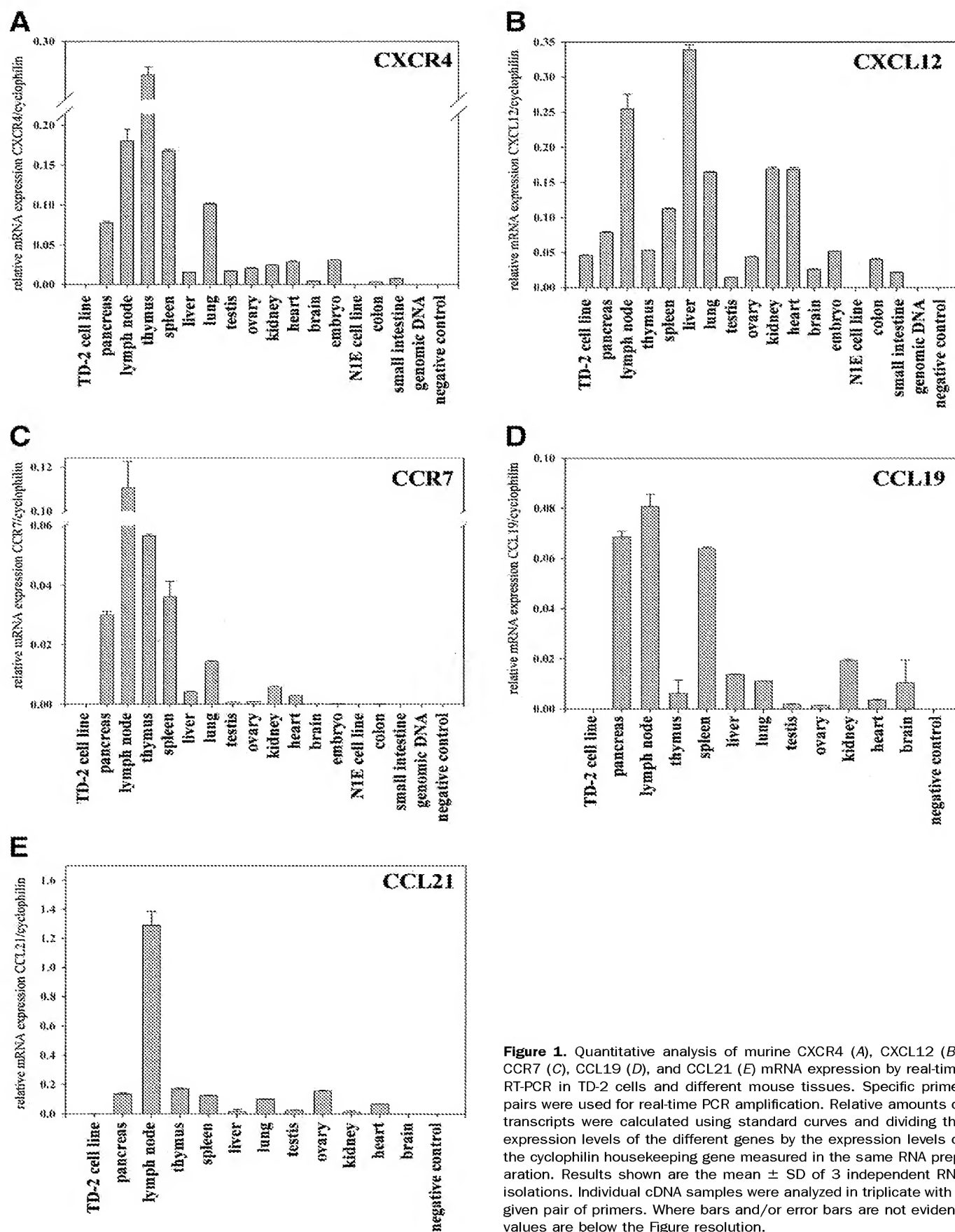
As demonstrated by quantitative RT-PCR, TD-2 cells show low expression levels of CXCR4 and CCR7. To evaluate the role of CXCR4 and CCR7 in targeted metastasis of pancreatic cancer cells in vitro

and in vivo, we generated TD-2 cell clones with stable CXCR4 and CCR7 expression, respectively. To monitor tumor growth and metastasis in vivo using bioluminescence imaging, cells were transfected with a bicistronic expression cassette for fLuc/CXCR4 (TD-2 fLuc-CXCR4) and fLuc/CCR7 (TD-2 fLuc-CCR7), respectively. As control, TD-2 cells with expression of fLuc alone (TD-2 fLuc) were used. Clones with comparable high fLuc activities (Figure 2A) and CXCR4 mRNA expression levels, similar to those of human pancreatic cancer cell lines derived from metastatic lesions (Capan1, Hs766T; Figure 2B), were selected for further analysis. To confirm that CXCR4 and CCR7 expression resulted in functional proteins, cell surface expression was evaluated by flow cytometry, and functional chemokine receptor signaling was assessed by calcium flux assays. Flow cytometry revealed absence of CXCR4 and CCR7 cell surface expression in native and fLuc-expressing TD-2 cell lines, whereas TD-2 fLuc-CXCR4 (Figure 2C) and TD-2 fLuc-CCR7 (Figure 2E) cells were CXCR4 and CCR7 positive, respectively. Furthermore, TD-2 fLuc-CXCR4 cells showed similar cell surface expression levels of CXCR4 as the human cell line Hs766T, derived from a pancreatic cancer metastatic lesion (Figure 2D).

Binding of chemokines to their receptors results in a characteristic increase in cytosolic calcium levels. Therefore, functional expression of CXCR4 and CCR7 can be evaluated by fluorometric calcium mobilization assays. Stimulation of TD-2 fLuc-CXCR4 cells with CXCL12 (Figure 3A) and TD-2 fLuc-CCR7 cells with CCL21 (Figure 3B), respectively, resulted in a rapid increase of intracellular calcium demonstrating functional expression of CXCR4 and CCR7 proteins.

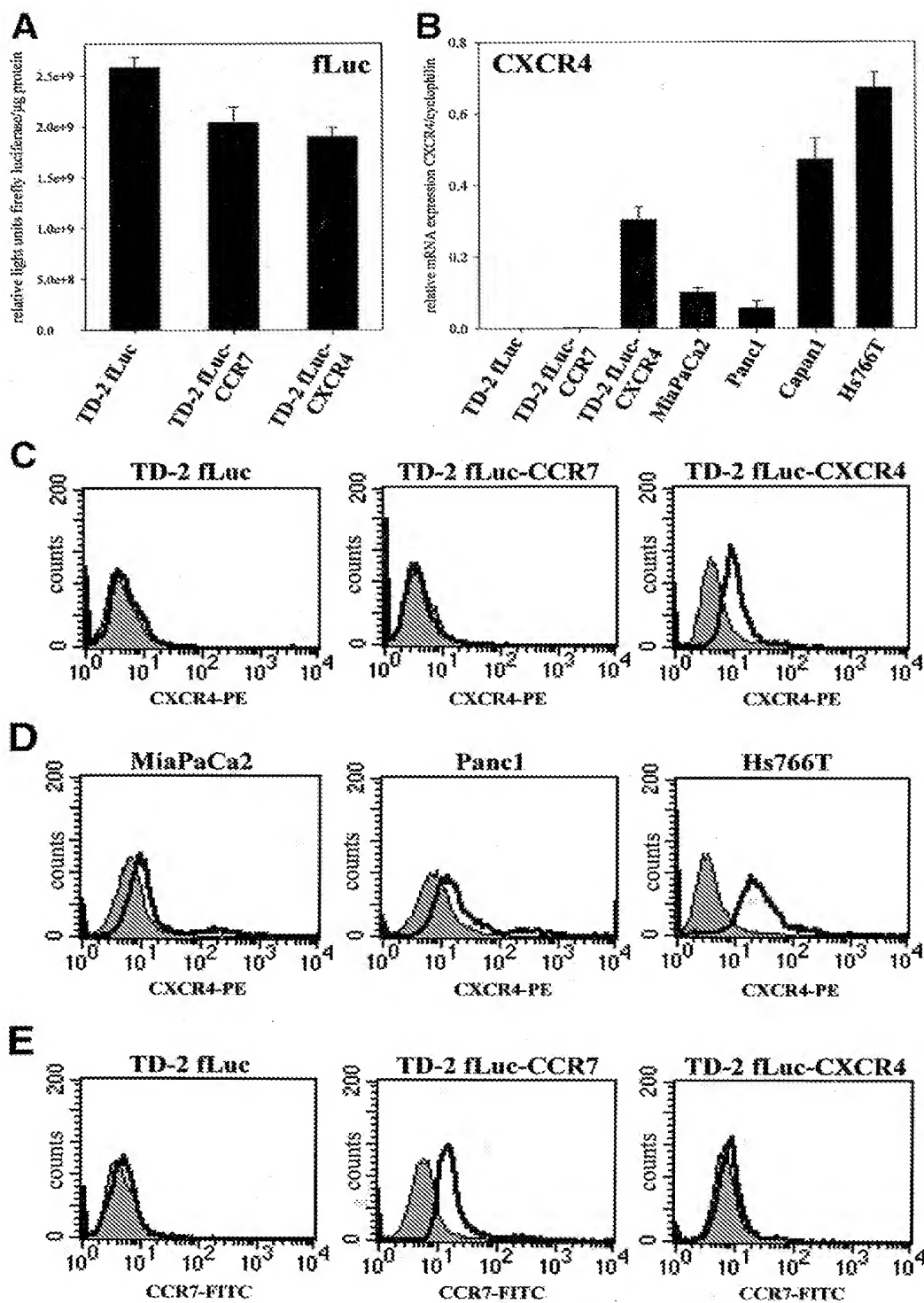
### Expression of CXCR4 Accelerates CXCL12-Induced Migration of Murine TD-2 Pancreatic Cancer Cells

To test whether interactions of CXCL12 with CXCR4 and CCL21 with CCR7 induce chemotaxis of pancreatic cancer cells, modified Boyden chamber assays were performed. Stimulation of TD-2 fLuc-CXCR4 cells with CXCL12 induced migration in a concentration-dependent manner (optimum concentration, 100 ng/mL). In contrast, native TD-2, TD-2-fLuc, and TD-2 fLuc-CCR7 cells did not migrate in response to CXCL12 (Figure 3C). Incubation of both native and stable transfected TD-2 cells (fLuc, fLuc-CXCR4, and fLuc-CCR7) with the CCR7 ligand CCL21 did not result in a chemotactic response (data not shown).



**Figure 1.** Quantitative analysis of murine CXCR4 (A), CXCL12 (B), CCR7 (C), CCL19 (D), and CCL21 (E) mRNA expression by real-time RT-PCR in TD-2 cells and different mouse tissues. Specific primer pairs were used for real-time PCR amplification. Relative amounts of transcripts were calculated using standard curves and dividing the expression levels of the different genes by the expression levels of the cyclophilin housekeeping gene measured in the same RNA preparation. Results shown are the mean  $\pm$  SD of 3 independent RNA isolations. Individual cDNA samples were analyzed in triplicate with a given pair of primers. Where bars and/or error bars are not evident, values are below the Figure resolution.

**Figure 2.** Firefly luciferase and CXCR4 expression in stable murine TD-2 cell clones and human pancreatic cancer cell lines. (A) Firefly luciferase activity of the indicated stable transfected TD-2 clones was assayed by using a luciferase assay system as described in the Materials and Methods section and normalized for total cellular protein values of lysed cells. The data are expressed as means  $\pm$  SD of 3 experiments in triplicate. (B) Quantitative analysis of murine and human CXCR4 mRNA expression by real-time RT-PCR. CXCR4 mRNA expression levels were quantified in stable transfected TD-2 cells with expression of firefly luciferase (*TD-2 fLuc*), firefly luciferase and CCR7 (*TD-2 fLuc-CCR7*), and firefly luciferase and CXCR4 (*TD-2 fLuc-CXCR4*), respectively. In addition, CXCR4 expression of human pancreatic cancer cell lines derived from primary tumors (*MiaPaCa2*, *Panc1*) and metastatic lesions (*Capan1*, *Hs766T*) was assessed. Specific murine and human CXCR4 primer pairs were used for real-time PCR amplification. CXCR4 mRNA expression was normalized against the housekeeping gene cyclophilin. Results shown are the mean  $\pm$  SD of 3 independent RNA isolations. Individual cDNA samples were analyzed in triplicate. Where bars and/or error bars are not evident, values are below the Figure resolution. (C–E) Flow cytometry of CXCR4 and CCR7 cell surface expression. (C) Stable transfected *TD-2 fLuc*, *TD-2 fLuc-CCR7*, and *TD-2 fLuc-CXCR4* cells were stained with phycoerythrin (PE) labeled anti-mouse CXCR4 antibody or isotype control as described in the Materials and Methods section. Flow cytometry demonstrated cell surface expression of murine CXCR4 in stable *TD-2 fLuc-CXCR4* but not in *TD-2 fLuc* and *TD-2 fLuc-CCR7* cells. (D) Human pancreatic cancer cell lines derived from primary tumors (*MiaPaCa2*, *Panc1*) and metastatic lesions (*Hs766T*) were stained with PE-labeled anti-human CXCR4 antibody. Cell surface expression of CXCR4 was highest in metastatic *Hs766T* cells. (E) Stable transfected *TD-2 fLuc*, *TD-2 fLuc-CCR7*, and *TD-2 fLuc-CXCR4* cells were stained with anti-mouse CCR7 antibody. FITC-conjugated anti-goat IgG was used as secondary antibody. *TD-2 fLuc-CCR7*, but not *TD-2 fLuc* and *TD-2 fLuc-CXCR4*, cells showed CCR7 cell surface expression.



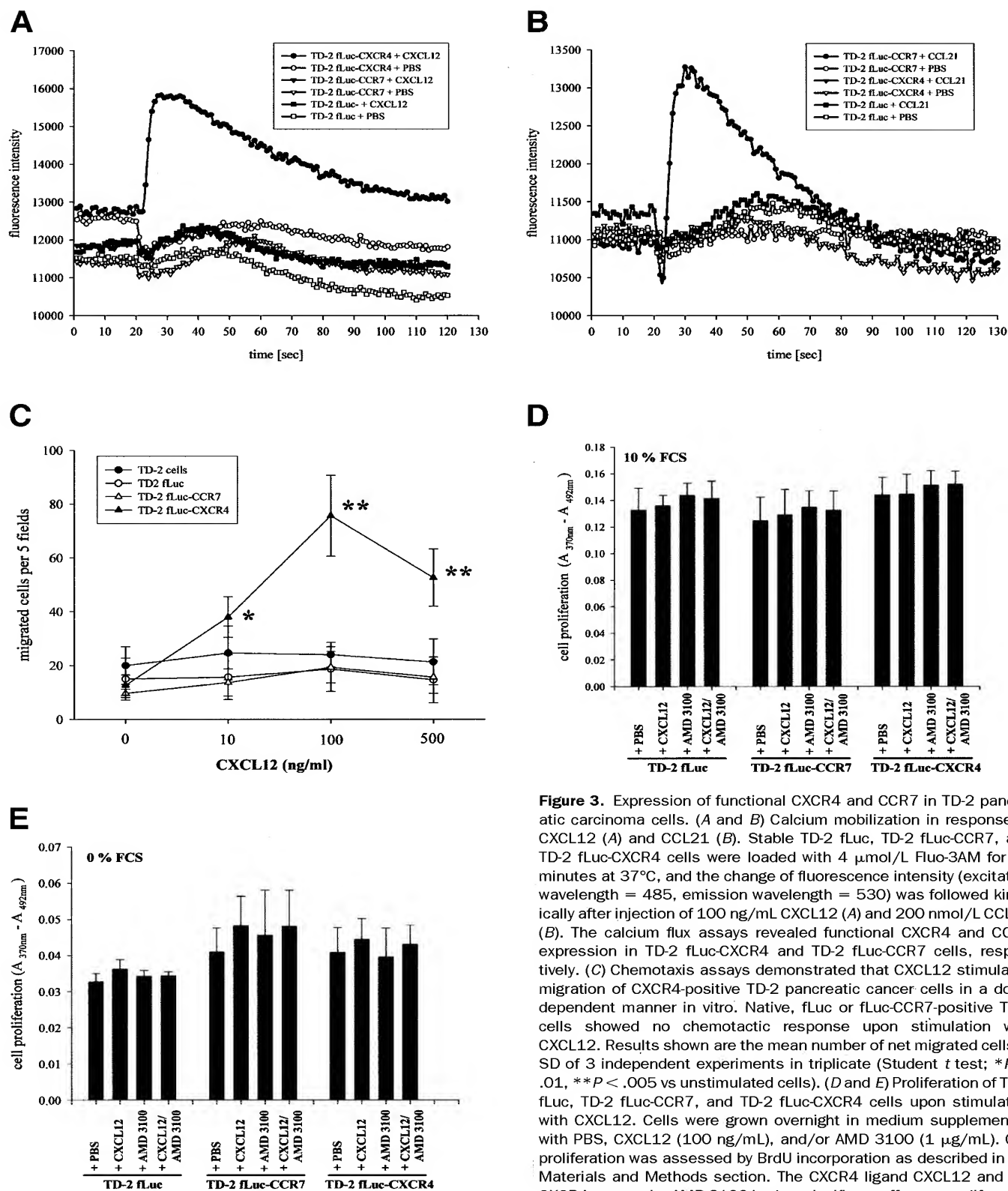


**Figure 3.** Expression of functional CXCR4 and CCR7 in TD-2 pancreatic carcinoma cells. (A and B) Calcium mobilization in response to CXCL12 (A) and CCL21 (B). Stable TD-2 fLuc, TD-2 fLuc-CCR7, and TD-2 fLuc-CXCR4 cells were loaded with 4  $\mu$ M Fluo-3AM for 60 minutes at 37°C, and the change of fluorescence intensity (excitation wavelength = 485, emission wavelength = 530) was followed kinetically after injection of 100 ng/mL CXCL12 (A) and 200 nmol/L CCL21 (B). The calcium flux assays revealed functional CXCR4 and CCR7 expression in TD-2 fLuc-CXCR4 and TD-2 fLuc-CCR7 cells, respectively. (C) Chemotaxis assays demonstrated that CXCL12 stimulates migration of CXCR4-positive TD-2 pancreatic cancer cells in a dose-dependent manner in vitro. Native, fLuc or fLuc-CCR7-positive TD-2 cells showed no chemotactic response upon stimulation with CXCL12. Results shown are the mean number of net migrated cells  $\pm$  SD of 3 independent experiments in triplicate (Student *t* test; \**P* < .01, \*\**P* < .005 vs unstimulated cells). (D and E) Proliferation of TD-2 fLuc, TD-2 fLuc-CCR7, and TD-2 fLuc-CXCR4 cells upon stimulation with CXCL12. Cells were grown overnight in medium supplemented with PBS, CXCL12 (100 ng/mL), and/or AMD 3100 (1  $\mu$ g/mL). Cell proliferation was assessed by BrdU incorporation as described in the Materials and Methods section. The CXCR4 ligand CXCL12 and the CXCR4 antagonist AMD 3100 had no significant effect on proliferation of the different cell clones cultured in medium containing 10% FCS (D) and 0% FCS (E). Results are expressed as mean of the absorbance ( $A_{370nm} - A_{492nm}$ ) of stimulated and unstimulated cells  $\pm$  SD from 3 independent experiments in triplicate.

### **Expression of CXCR4 Has No Effect on TD-2 Pancreatic Cancer Cell Proliferation and Viability**

Controversial results have been reported concerning the impact of CXCR4 receptor activation on human pancreatic cancer cell proliferation.<sup>23,24</sup> Therefore, we evaluated the effect of CXCL12 stimulation on proliferation of murine TD-2 cells by BrdU and MTT assays. TD-2 cells depend on serum for maximal growth under cell culture conditions. Thus, proliferation of the different stable TD-2 clones was tested under optimal conditions (10% FCS), suboptimal conditions (1% FCS), and without serum (0% FCS). Under optimal serum conditions, proliferation of the different TD-2 cell clones was identical with and without addition of CXCL12 (Figure 3D). Furthermore, addition of the selective noncompetitive CXCR4 antagonist AMD 3100, which blocks binding of CXCL12 to CXCR4,<sup>34</sup> did not change the proliferation rate of the different TD-2 clones, excluding an autocrine growth-regulating loop (Figure 3D). Similar results were obtained for suboptimal serum conditions (1% FCS, data not shown) and 0% FCS (Figure 3E). Therefore, expression of CXCR4 has no effect on proliferation of CXCL12-stimulated TD-2 cells *in vitro*. In addition, no differences in cell viability were observed between the different TD-2 cell clones after addition of CXCL12 and/or AMD 3100 as assessed by MTT assays (data not shown).

### **Expression of CXCR4 Mediates Liver and Accelerates Lung Metastasis of Murine Pancreatic Cancer Cells *In Vivo***

To assess the effect of CXCR4 and CCR7 expression for organ-specific metastasis of TD-2 pancreatic cancer cells *in vivo*, tail vein metastatic assays were performed. Stable TD-2 transfectants, expressing fLuc (control cell line), fLuc and CCR7, and fLuc and CXCR4 were injected IV into nude mice, and metastasis was monitored by noninvasive imaging of tumor-associated bioluminescence *in vivo*. Mice were killed after 120 days, or at the time when metastasis was demonstrated by bioluminescent imaging, and tissues were examined macroscopically and microscopically for occurrence of metastases (Figure 4). TD-2 fLuc cells displayed poor metastatic potential after IV injection into nude mice. Only 2 of 14 mice developed pulmonary metastases, and none of 14 developed liver metastases as shown in Table 2. Expression of CXCR4, but not CCR7, dramatically enhanced the metastatic potential of TD-2 cells, resulting in the formation of lung and/or liver metastases in 12 of 14 injected mice (Table 2). Metastasis was assessed by

*in vivo* bioluminescence imaging (Figure 4A, E, I, and L), *ex vivo* bioluminescence imaging (Figure 4B, C, J, K, and N), macroscopic pathologic examination (Figure 4F and M), H&E staining (Figures 4D, G, H and 5A, D, G, and J), and semiquantitative real-time RT-PCR for fLuc and CXCR4 (data not shown). Proliferation of TD-2 fLuc-CXCR4-derived metastatic lesions could be demonstrated by proliferating cell nuclear antigen staining (Figure 5B and E) and maintenance of CXCR4 expression *in vivo* by CXCR4 immunohistochemistry (Figure 5C and F) and real-time RT-PCR (data not shown). TD-2 fLuc and TD-2 fLuc-CCR7-derived pulmonary metastases were CXCR4 negative (Figure 5I and L) and showed a PCNA staining pattern similar to that of TD-2 fLuc-CXCR4 cells (Figure 5B, E, H, and K). After more than 3 months, all mice developed macroscopically visible subcutaneous tumors at the site of IV injection, indicating tumorigenicity of the injected cell clones. In addition, the size of the subcutaneous tail tumors was not statistically significant different among the 3 groups (TD-2 fLuc, TD-2 fLuc-CCR7, and TD-2 fLuc-CXCR4 injected mice) as determined by quantification of luciferase activity and tumor volume (data not shown). These findings regarding PCNA expression and tumor volume confirm our *in vitro* data that CXCR4 expression has no effect on proliferation of murine TD-2 pancreatic cancer cells (Figure 3B). Taken together, these results clearly show that expression of the chemokine receptor CXCR4 increases the pulmonary metastatic potential of TD-2 cells substantially and indicate that CXCR4 mediates liver metastasis *in vivo*.

### **The Specific CXCR4 Antagonist AMD 3100 Inhibits the Enhanced Metastatic Potential of CXCR4-Positive TD-2 Cells *In Vivo***

To test whether the bicyclam AMD 3100 can inhibit CXCR4-mediated metastasis, nude mice were IV injected with TD-2 fLuc-CXCR4 cells and treated with either AMD 3100 (1.25 mg/kg subcutaneously [SC] twice per day) or PBS as control for 10 days. The enhanced metastatic potential of TD-2 fLuc-CXCR4 cells was reversed by AMD 3100 treatment to levels seen in TD-2 fLuc and TD-2 fLuc-CCR7 injected mice, whereas it was unchanged in PBS-treated animals (Table 2). Treatment with AMD 3100 had no significant effect on the size of the subcutaneous tail tumors compared with PBS-treated animals. Therefore, AMD 3100 blocks metastasis of CXCR4-positive TD-2 pancreatic carcinoma cells but not tumor growth at the IV injection site.

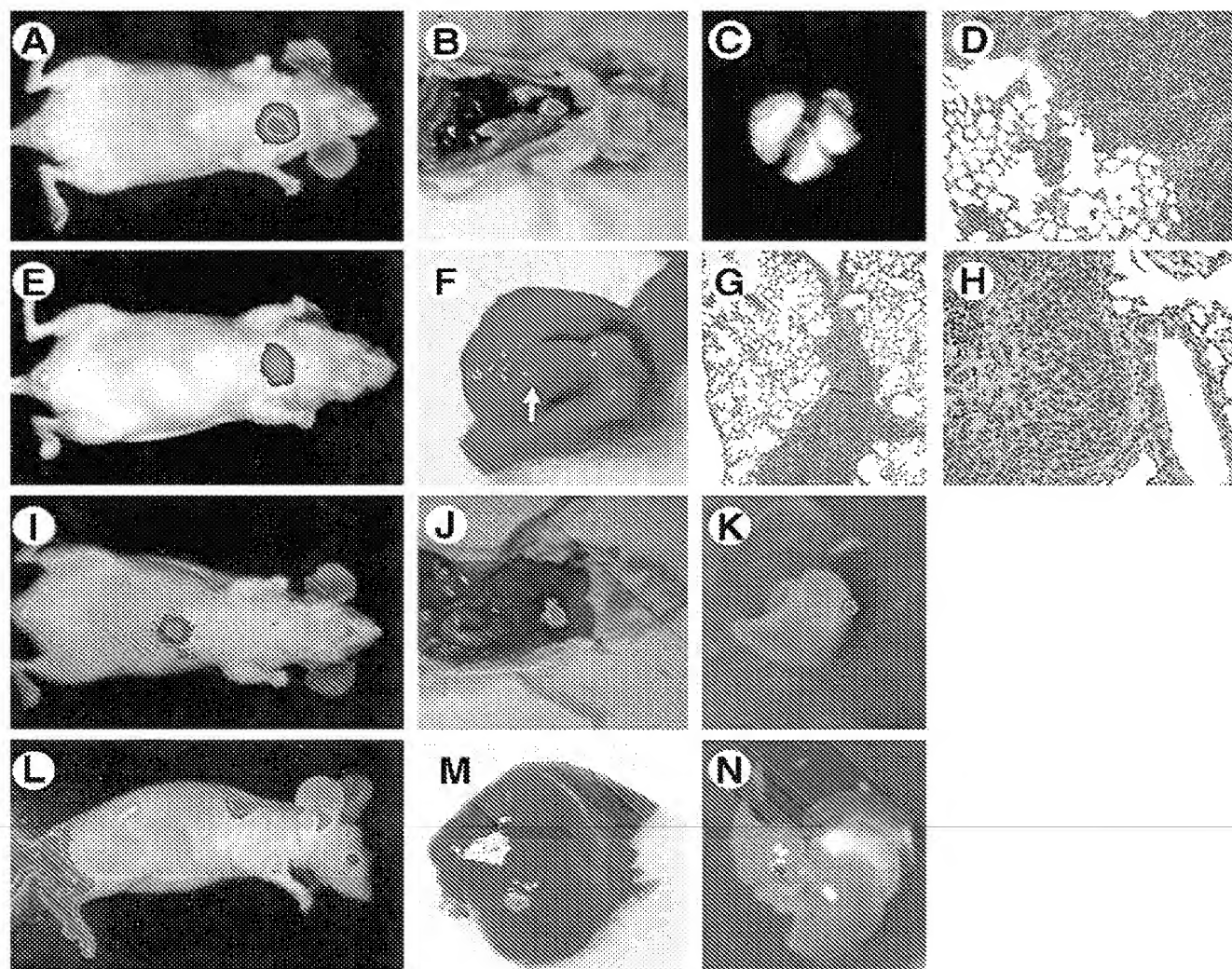


**Figure 4.** Effect of CXCR4 expression on liver and lung metastasis in vivo. Murine TD-2 pancreatic carcinoma cells were injected into the tail vein of nude mice. In vivo bioluminescence imaging of organ-specific metastasis of CXCR4 expressing TD-2 cells to the lung (A and E) and to the liver (I and L). Detection of metastatic sites in the lung (B and C) and the liver (J, K, and N) ex vivo by using bioluminescence imaging. Macroscopic images of metastatic lesions in the lung (F) and the liver (M). H&E staining of lungs from nude mice with metastatic lesions (D, G, and H).

## Discussion

Metastasis is the main cause of cancer death in the Western world. However, the mechanisms of organ-specific metastasis are largely unknown. The results of this study show that expression of chemokine receptor CXCR4 dramatically increases liver and lung metastasis of murine TD-2 pancreatic cancer cells in vivo and define CXCR4 as a key mediator of organ-specific metastasis. The role of CXCR4 expression for targeted metastasis was investigated in a mouse model using pancreatic cancer cells with stable expression of fLuc and similar expression levels of CXCR4 as human pancreatic cancer cell lines derived from metastatic lesions. By using non-invasive bioluminescent imaging, this model allows

monitoring of tumor progression and organ-specific metastasis in vivo in the same cohort of mice. For this reason, it is an important tool to evaluate novel antitumor or antimetastatic treatment strategies. Using this model, we demonstrate here that blockade of CXCR4 by the specific antagonist AMD 3100 blocks targeted metastasis, and, therefore, we provide preclinical data that the CXCL12/CXCR4 axis is a potential target for antimetastatic pancreatic cancer therapy.

In contrast to CXCR4, signaling by CCR7 does not result in enhanced hematogenous metastasis in our model. Recent work supports this observation. Wiley et al showed that over expression of CCR7 accelerates lymphatic, but not hematogenous, metastasis,<sup>21</sup> whereas



**Table 2.** In Vivo Metastatic Potential of Stable TD-2 Pancreatic Cancer Cells With Expression of Firefly Luciferase and CXCR4 (TD-2 fLuc-CXCR4), Firefly Luciferase and CCR7 (TD-2 fLuc-CCR7), and, as Control, Firefly Luciferase Alone (TD-2 fLuc)

Cell line	Tumorigenicity	Frequency (metastasis/total)	Lung (metastasis/total)	Liver (metastasis/total)
TD-2 fLuc-CXCR4	14/14	12/14**	9/14**	4/14*
TD-2 fLuc-CCR7	14/14	4/14	4/14	0/14
TD-2 fLuc	14/14	2/14	2/14	0/14
TD-2 fLuc-CXCR4 + AMD 3100	7/7	1/7†	1/7†	0/7 <sup>ns</sup>
TD-2 fLuc-CXCR4 + PBS	7/7	6/7	5/7	2/7

NOTE. Experimental tail vein metastatic assays were performed to determine the in vivo metastatic potential of the different TD-2 pancreatic cancer cell clones. Mice were killed not later than 120 days after IV injection of the tumor cells. Metastatic lesions were determined by in vivo bioluminescence imaging and pathologic examination. Comparisons between each group were made by Fisher exact test (\*\* $P < .01$ , \* $P < .05$  compared with TD-2 fLuc).

The effect of the specific CXCR4 antagonist AMD 3100 was investigated in vivo. AMD 3100 (1.25 mg/kg) or PBS as control was administered subcutaneously twice per day for 10 days and metastatic lesions were examined. Comparison between the treatment groups was made by Fisher exact test. † $P < .05$ , compared with TD-2 fLuc-CXCR4 + PBS.

CXCR4 expression increases pulmonary metastasis in an experimental model of melanoma.<sup>20</sup> Moreover, expression of CXCR4 leads to similar metastatic signatures of different cancer types. The liver and/or the lung are the common target organs of CXCR4-mediated metastasis in animal models of melanoma, breast, prostate, and colon cancer<sup>15–20</sup> and in our model of pancreatic cancer. These results demonstrate that different chemokine receptors mediate organ-specific metastatic signatures and are able to alter the metastatic fate of cancer cells.

In human pancreatic cancer, CXCR4 is over-expressed in cell lines derived from metastatic lesions, whereas those derived from primary tumors show lower expression levels.<sup>24</sup> CXCR4 signaling results in increased survival, proliferation, invasion, and migration of these cell lines in vitro,<sup>24</sup> indicating that CXCR4 may play a major role for pancreatic tumor progression, invasion, and metastasis in vivo. However, as experimental data observed in vitro do not always correlate with in vivo findings, the relevance and distinct role of CXCR4 expression for the multiple steps toward metastasis of pancreatic cancer cells in living organisms remain unclear. Our study provides evidence that CXCR4 expression induces chemotaxis of murine TD-2 pancreatic cancer cells and thus promotes liver and lung metastasis without affecting tumor cell growth. We observed an unchanged proliferation rate of CXCR4-positive TD-2 cells in vitro during CXCL12 stimulation and in vivo after inhibition of CXCR4 with the specific antagonist AMD 3100. This is in line with a recent study demonstrating an unchanged proliferation rate of the human pancreatic cancer cell lines ASPC1, Panc1, and Suit-2 under CXCL12 stimulation.<sup>23</sup> In contrast, CXCL12 increased cell proliferation of the human pancreatic cancer cell lines ASPC1 and Hs766T in vitro under serum-free culture conditions in another study.<sup>24</sup> It has been shown that CXCL12 stim-

ulates proliferation of different cell types through CXCR4-dependent activation of the p44/p42 MAPK/extracellular signal-regulated kinase 1/2, the phosphatidylinositol 3-kinase/Akt, and the Src-kinase pathways.<sup>35–38</sup> Therefore, the unchanged proliferation rate observed in our study may be due to constitutive activation of these pathways in TD-2 cells. We have shown previously that some of these pathways are already activated in pancreatic carcinomas of TGF- $\alpha$ /p53<sup>+/-</sup> mice and TD-2 cells,<sup>26,30</sup> and, therefore, signaling by CXCR4 may not further enhance these mitogenic pathways.

CXCL12 is constitutively expressed and locally secreted in selected tissues, including lymph nodes, liver, and lung, which are the major homing organs of pancreatic cancer cells. However, both CXCR4 and CXCL12 are also expressed at lower levels in the murine pancreas as demonstrated by semiquantitative real-time RT-PCR. These results are in line with a recent study by Kayali et al, showing expression of CXCR4 and CXCL12 in fetal pancreatic islets and in proliferating duct epithelium during pancreatic regeneration of interferon- $\gamma$  nonobese diabetic mice.<sup>35</sup> In these mice, CXCL12/CXCR4 signaling induces proliferation and migration of pancreatic duct and/or progenitor cells in vivo by stimulation of Akt, mitogen-activated protein kinase and Src phosphorylation. Therefore, the CXCL12/CXCR4 chemotactic axis is a critical survival and regeneration factor of nonmalignant pancreatic duct and/or precursor cells.

CXCR4 is a target gene of transcription factors such as HIF1 $\alpha$ <sup>39,40</sup> or NF- $\kappa$ B<sup>41</sup> and signaling pathways activated by VEGF,<sup>42</sup> HER2/ErbB-2/Neu,<sup>16</sup> RET/PTC,<sup>43</sup> PAX3-FKHR fusion oncoprotein,<sup>44</sup> and TGF- $\beta$ ,<sup>45</sup> all known to be involved in carcinogenesis. Seventy percent to 80% of infiltrating human ductal pancreatic carcinomas overexpress HER2/ErbB-2/Neu.<sup>46–49</sup> In addition, expression

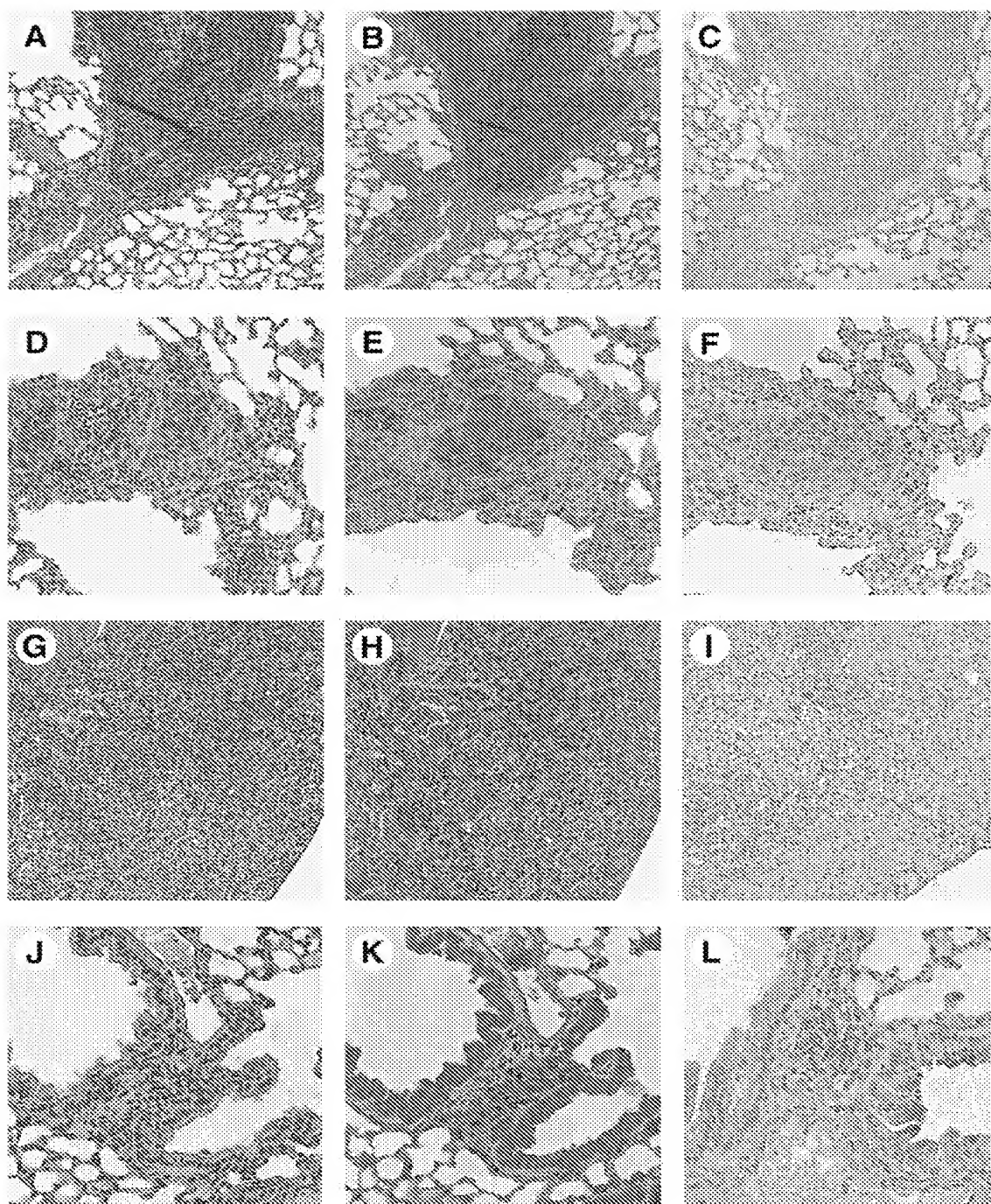


**Figure 5.** Histochemistry of metastatic lesions upon intravenous administration of TD-2 pancreatic cancer cells to nude mice. (A–F) CXCR4-positive TD-2 cells were injected into nude mice. Pulmonary metastases were stained by H&E (A and D). Immunohistochemistry for PCNA (B and E) and CXCR4 (C and F) demonstrates proliferation and maintenance of CXCR4 expression of pulmonary metastatic lesions, respectively. (G–L) CXCR4-negative TD-2 cells (TD-2 fluc) were injected into nude mice. H&E staining of pulmonary metastases (G and J). Immunohistochemistry for PCNA (H and K) and CXCR4 (I and L) demonstrates proliferation and absence of CXCR4 expression of lung metastases derived from TD-2 fluc cells. (A–C, G–I: Magnification  $\times 100$ ; D–F, J–L: Magnification  $\times 200$ ).

of HER2/ErbB-2/Neu was observed in 55%–92% of early premalignant pancreatic duct lesions, known as pancreatic intraepithelial neoplasias (PanIN lesions). HER2/ErbB-2/Neu enhances CXCR4 expression and in-

hibits ligand-induced CXCR4 degradation in human breast cancer.<sup>16</sup> Therefore, acquisition of CXCR4 expression might occur in early pancreatic cancer lesions and may provide these cells with a distinct repertoire of key



prometastatic features. This might explain in part the micrometastatic behavior of the disease.

The importance of the CXCL12/CXCR4 chemotactic axis for pancreatic cancer metastasis was directly demonstrated in our study through the antimetastatic activity of AMD 3100. This small molecule antagonist of CXCR4 completely blocked the dramatically enhanced metastatic potential of CXCR4-expressing TD-2 cells *in vivo*. Taken together, our data provide preclinical evidence that AMD 3100 or other CXCR4 inhibitors, such as T22,<sup>22,50</sup> may have an important role as antimetastatic drugs and therefore provide the scientific rationale for the evaluation of CXCR4 antagonists in controlled clinical trials of adjuvant pancreatic cancer therapies.

## References

- Jemal A, Tiwari RC, Murray T, Ghafoor A, Samuels A, Ward E, Feuer EJ, Thun MJ. Cancer statistics, 2004. *CA Cancer J Clin* 2004;54:8–29.
- Warshaw AL, Fernandez-del Castillo C. Pancreatic carcinoma. *N Engl J Med* 1992;326:455–465.
- Ahrendt SA, Pitt HA. Surgical management of pancreatic cancer. *Oncology* 2002;16:725–734.
- Neoptolemos JP, Stocken DD, Friess H, Bassi C, Dunn JA, Hickey H, Beger H, Fernandez-Cruz L, Dervenis C, Lacaine F, Falconi M, Pederzoli P, Pap A, Spooner D, Kerr DJ, Buchler MW. A randomized trial of chemoradiotherapy and chemotherapy after resection of pancreatic cancer. *N Engl J Med* 2004;350:1200–1210.
- Weiss L. Comments on hematogenous metastatic patterns in humans as revealed by autopsy. *Clin Exp Metastasis* 1992;10:191–199.
- Hynes RO. Metastatic potential: generic predisposition of the primary tumor or rare, metastatic variants—or both? *Cell* 2003;113:821–823.
- Fidler IJ. The pathogenesis of cancer metastasis: the “seed and soil” hypothesis revisited. *Nat Rev Cancer* 2003;3:453–458.
- Liotta LA. An attractive force in metastasis. *Nature* 2001;410:24–25.
- Chambers AF, Groom AC, MacDonald IC. Dissemination and growth of cancer cells in metastatic sites. *Nat Rev Cancer* 2002;2:563–572.
- Keleg S, Buchler P, Ludwig R, Buchler MW, Friess H. Invasion and metastasis in pancreatic cancer. *Mol Cancer* 2003;2:14.
- Zlotnik A. Chemokines in neoplastic progression. *Semin Cancer Biol* 2004;14:181–185.
- Forster R, Ohl L, Henning G. Lessons learned from lymphocytes: CC chemokine receptor-7 involved in lymphogenic metastasis of melanoma. *J Natl Cancer Inst* 2001;93:1588–1589.
- Strieter RM. Chemokines: not just leukocyte chemoattractants in the promotion of cancer. *Nat Immunol* 2001;2:285–286.
- Zlotnik A, Yoshie O. Chemokines: a new classification system and their role in immunity. *Immunity* 2000;12:121–127.
- Muller A, Homey B, Soto H, Ge N, Catron D, Buchanan ME, McClanahan T, Murphy E, Yuan W, Wagner SN, Barrera JL, Mohar A, Verastegui E, Zlotnik A. Involvement of chemokine receptors in breast cancer metastasis. *Nature* 2001;410:50–56.
- Li YM, Pan Y, Wei Y, Cheng X, Zhou BP, Tan M, Zhou X, Xia W, Hortobagyi GN, Yu D, Hung MC. Up-regulation of CXCR4 is essential for HER2-mediated tumor metastasis. *Cancer Cell* 2004;6:459–469.
- Zeelenberg IS, Ruuls-Van Stalle L, Roos E. The chemokine receptor CXCR4 is required for outgrowth of colon carcinoma micrometastases. *Cancer Res* 2003;63:3833–3839.
- Taichman RS, Cooper C, Keller ET, Pienta KJ, Taichman NS, McCauley LK. Use of the stromal cell-derived factor-1/CXCR4 pathway in prostate cancer metastasis to bone. *Cancer Res* 2002;62:1832–1837.
- Darash-Yahana M, Pikarsky E, Abramovitch R, Zeira E, Pal B, Karplus R, Beider K, Avniel S, Kasem S, Galun E, Peled A. Role of high expression levels of CXCR4 in tumor growth, vascularization, and metastasis. *FASEB J* 2004;18:1240–1242.
- Murakami T, Maki W, Cardones AR, Fang H, Tun KA, Nestle FO, Hwang ST. Expression of CXC chemokine receptor-4 enhances the pulmonary metastatic potential of murine B16 melanoma cells. *Cancer Res* 2002;62:7328–7334.
- Wiley HE, Gonzalez EB, Maki W, Wu MT, Hwang ST. Expression of CC chemokine receptor-7 and regional lymph node metastasis of B16 murine melanoma. *J Natl Cancer Inst* 2001;93:1638–1643.
- Koshiba T, Hosotani R, Miyamoto Y, Ida J, Tsuji S, Nakajima S, Kawaguchi M, Kobayashi H, Doi R, Hori T, Fujii N, Imamura M. Expression of stromal cell-derived factor 1 and CXCR4 ligand receptor system in pancreatic cancer: a possible role for tumor progression. *Clin Cancer Res* 2000;6:3530–3535.
- Mori T, Doi R, Koizumi M, Toyoda E, Ito D, Kami K, Masui T, Fujimoto K, Tamamura H, Hiramatsu K, Fujii N, Imamura M. CXCR4 antagonist inhibits stromal cell-derived factor 1-induced migration and invasion of human pancreatic cancer. *Mol Cancer Ther* 2004;3:29–37.
- Marchesi F, Monti P, Leone BE, Zerbi A, Vecchi A, Piemonti L, Mantovani A, Allavena P. Increased survival, proliferation, and migration in metastatic human pancreatic tumor cells expressing functional CXCR4. *Cancer Res* 2004;64:8420–8427.
- Greten FR, Weber CK, Greten TF, Schneider G, Wagner M, Adler G, Schmid RM. Stat3 and NF- $\kappa$ B activation prevents apoptosis in pancreatic carcinogenesis. *Gastroenterology* 2002;123:2052–2063.
- Schreiner B, Greten FR, Baur DM, Fingerle AA, Zechner U, Bohm C, Schmid M, Hameister H, Schmid RM. Murine pancreatic tumor cell line TD2 bears the characteristic pattern of genetic changes with two independently amplified gene loci. *Oncogene* 2003;22:6802–6809.
- Saur D, Paehge H, Schusdziarra V, Allescher HD. Distinct expression of splice variants of neuronal nitric oxide synthase in the human gastrointestinal tract. *Gastroenterology* 2000;118:849–858.
- Saur D, Neuhuber WL, Gengenbach B, Huber A, Schusdziarra V, Allescher HD. Site-specific gene expression of nNOS variants in distinct functional regions of rat gastrointestinal tract. *Am J Physiol Gastrointest Liver Physiol* 2002;282:G349–G358.
- Saur D, Seidler B, Paehge H, Schusdziarra V, Allescher HD. Complex regulation of human neuronal nitric-oxide synthase exon 1c gene transcription. Essential role of Sp and ZNF family members of transcription factors. *J Biol Chem* 2002;277:25798–25814.
- Wagner M, Greten FR, Weber CK, Koschnick S, Mattfeldt T, Deppert W, Kern H, Adler G, Schmid RM. A murine tumor progression model for pancreatic cancer recapitulating the genetic alterations of the human disease. *Genes Dev* 2001;15:286–293.
- Saur D, Vanderwinden JM, Seidler B, Schmid RM, De Laet MH, Allescher HD. Single-nucleotide promoter polymorphism alters transcription of neuronal nitric oxide synthase exon 1c in infantile hypertrophic pyloric stenosis. *Proc Natl Acad Sci U S A* 2004;101:1662–1667.
- Lin K, Sadee W, Quillan JM. Rapid measurements of intracellular calcium using a fluorescence plate reader. *Biotechniques* 1999;26:318–322.

33. Elkin M, Vlodavsky I. Tail vein assay of cancer metastasis. In: Bonifacino JS, Dasso M, Lippincott-Schwartz J, Harford JB, Yamada KM, eds. *Current protocols in cell biology*. New York: John Wiley & Sons, 2001:Unit 19.2.
34. Gerlach LO, Skerlj RT, Bridger GJ, Schwartz TW. Molecular interactions of cyclam and bicyclam non-peptide antagonists with the CXCR4 chemokine receptor. *J Biol Chem* 2001;276:14153–14160.
35. Kayali AG, Van Gunst K, Campbell IL, Stotland A, Kritzik M, Liu G, Flodstrom-Tullberg M, Zhang YQ, Sarvetnick N. The stromal cell-derived factor-1 $\alpha$ /CXCR4 ligand-receptor axis is critical for progenitor survival and migration in the pancreas. *J Cell Biol* 2003;163:859–869.
36. Rubin JB, Kung AL, Klein RS, Chan JA, Sun Y, Schmidt K, Kieran MW, Luster AD, Segal RA. A small-molecule antagonist of CXCR4 inhibits intracranial growth of primary brain tumors. *Proc Natl Acad Sci U S A* 2003;100:13513–13518.
37. Barbero S, Bonavia R, Bajetto A, Porcile C, Pirani P, Ravetti JL, Zona GL, Spaziante R, Florio T, Schettini G. Stromal cell-derived factor 1 $\alpha$  stimulates human glioblastoma cell growth through the activation of both extracellular signal-regulated kinases 1/2 and Akt. *Cancer Res* 2003;63:1969–1974.
38. Suzuki Y, Rahman M, Mitsuya H. Diverse transcriptional response of CD4(+) T cells to stromal cell-derived factor (SDF)-1: cell survival promotion and priming effects of SDF-1 on CD4(+) T cells. *J Immunol* 2001;167:3064–3073.
39. Staller P, Sulitkova J, Lisztwan J, Moch H, Oakeley EJ, Krek W. Chemokine receptor CXCR4 down-regulated by von Hippel-Lindau tumour suppressor pVHL. *Nature* 2003;425:307–311.
40. Schioppa T, Uranchimeg B, Saccani A, Biswas SK, Doni A, Rapisarda A, Bernasconi S, Saccani S, Nebuloni M, Vago L, Mantovani A, Melillo G, Sica A. Regulation of the chemokine receptor CXCR4 by hypoxia. *J Exp Med* 2003;198:1391–1402.
41. Helbig G, Christopherson KW, Bhat-Nakshatri P, Kumar S, Kishimoto H, Miller KD, Broxmeyer HE, Nakshatri H. NF- $\kappa$ B promotes breast cancer cell migration and metastasis by inducing the expression of the chemokine receptor CXCR4. *J Biol Chem* 2003;278:21631–21638.
42. Bachelder RE, Wendt MA, Mercurio AM. Vascular endothelial growth factor promotes breast carcinoma invasion in an autocrine manner by regulating the chemokine receptor CXCR4. *Cancer Res* 2002;62:7203–7206.
43. Castellone MD, Guarino V, De Falco V, Carlomagno F, Basolo F, Faviana P, Kruhoffer M, Orntoft T, Russell JP, Rothstein JL, Fusco A, Santoro M, Melillo RM. Functional expression of the CXCR4 chemokine receptor is induced by RET/PTC oncogenes and is a common event in human papillary thyroid carcinomas. *Oncogene* 2004;23:5958–5967.
44. Tomescu O, Xia SJ, Strezlecki D, Bennicelli JL, Ginsberg J, Pawel B, Barr FG. Inducible short-term and stable long-term cell culture systems reveal that the PAX3-FKHR fusion oncoprotein regulates CXCR4, PAX3, and PAX7 expression. *Lab Invest* 2004;84:1060–1070.
45. Roes J, Choi BK, Cazac BB. Redirection of B cell responsiveness by transforming growth factor- $\beta$  receptor. *Proc Natl Acad Sci U S A* 2003;100:7241–7246.
46. Day JD, Diguseppe JA, Yeo C, LaiGoldman M, Anderson SM, Goodman SN, Kern SE, Hruban RH. Immunohistochemical evaluation of HER-2/neu expression in pancreatic adenocarcinoma and pancreatic intraepithelial neoplasms. *Hum Pathol* 1996;27:119–124.
47. Wilentz RE, Iacobuzio-Donahue CA, Argani P, McCarthy DM, Parsons JL, Yeo CJ, Kern SE, Hruban RH. Loss of expression of Dpc4 in pancreatic intraepithelial neoplasia: evidence that DPC4 inactivation occurs late in neoplastic progression. *Cancer Res* 2000;60:2002–2006.
48. Hruban RH, Wilentz RE, Kern SE. Genetic progression in the pancreatic ducts: commentary. *Am J Pathol* 2000;156:1821–1825.
49. Apple SK, Hecht JR, Lewin DN, Jahromi SA, Grody WW, Nieberg RK. Immunohistochemical evaluation of K-ras, p53, and HER-2/neu expression in hyperplastic, dysplastic, and carcinomatous lesions of the pancreas: evidence for multistep carcinogenesis. *Hum Pathol* 1999;30:123–129.
50. Murakami T, Nakajima T, Koyanagi Y, Tachibana K, Fujii N, Tamamura H, Yoshida N, Waki M, Matsumoto A, Yoshie O, Kishimoto T, Yamamoto N, Nagasawa T. A small molecule CXCR4 inhibitor that blocks T-cell line-tropic HIV-1 infection. *J Exp Med* 1997;186:1389–1393.

---

Received April 2, 2005. Accepted June 16, 2005.

Address requests for reprints to: Dieter Saur, MD, Department of Internal Medicine 2, Klinikum rechts der Isar, Technical University of Munich, Ismaningerstr. 22, 81675 Munich, Germany. e-mail: Dieter.Saur@lrz.tu-muenchen.de.; fax: (49) 89-4140-7289.

Supported by Kommission für klinische Forschung Technical University of Munich 46-02 (to D.S.).

The authors thank U. Götz, M. Werb, C. Kellnberger, B. Kohnke-Ertl, and U. Schwaiger for excellent technical assistance, Dr R. Fritsch for his suggestions during the preparation of the manuscript, and Dr J. Siveke for assistance with flow cytometry.